University of Nebraska - Lincoln
DigitalCommons@University of Nebraska - Lincoln

Faculty Publications from the Department of Electrical and Computer Engineering

Electrical & Computer Engineering, Department of

3-11-2013

Distributed fiber-optic laser-ultrasound generation based on ghost-mode of tilted fiber Bragg gratings

Jiajun Tian
University of Nebraska–Lincoln

Qi Zhang
University of Nebraska–Lincoln

Ming Han
University of Nebraska–Lincoln, mhan@egr.msu.edu

Follow this and additional works at: https://digitalcommons.unl.edu/electricalengineeringfacpub

 Part of the Computer Engineering Commons, and the Electrical and Computer Engineering Commons

Tian, Jiajun; Zhang, Qi; and Han, Ming, "Distributed fiber-optic laser-ultrasound generation based on ghost-mode of tilted fiber Bragg gratings" (2013). *Faculty Publications from the Department of Electrical and Computer Engineering*. 244.
https://digitalcommons.unl.edu/electricalengineeringfacpub/244

This Article is brought to you for free and open access by the Electrical & Computer Engineering, Department of at DigitalCommons@University of Nebraska - Lincoln. It has been accepted for inclusion in Faculty Publications from the Department of Electrical and Computer Engineering by an authorized administrator of DigitalCommons@University of Nebraska - Lincoln.

Distributed fiber-optic laser-ultrasound generation based on ghost-mode of tilted fiber Bragg gratings

Jiajun Tian, Qi Zhang, and Ming Han*

Department of Electrical Engineering, University of Nebraska–Lincoln, Lincoln, Nebraska 68588, USA
*mhan3@unl.edu

Abstract: Active ultrasonic testing is widely used for medical diagnosis, material characterization and structural health monitoring. Ultrasonic transducer is a key component in active ultrasonic testing. Due to their many advantages such as small size, light weight, and immunity to electromagnetic interference, fiber-optic ultrasonic transducers are particularly attractive for permanent, embedded applications in active ultrasonic testing for structural health monitoring. However, current fiber-optic transducers only allow effective ultrasound generation at a single location of the fiber end. Here we demonstrate a fiber-optic device that can effectively generate ultrasound at multiple, selected locations along a fiber in a controllable manner based on a smart light tapping scheme that only taps out the light of a particular wavelength for laser-ultrasound generation and allow light of longer wavelengths pass by without loss. Such a scheme may also find applications in remote fiber-optic device tuning and quasi-distributed biochemical fiber-optic sensing.

©2013 Optical Society of America

OCIS codes: (060.3735) Fiber Bragg gratings; (120.4290) Nondestructive testing.

References and links

1. L. Wang, *Photoacoustic Imaging and Spectroscopy* (CRC Press, 2009).
2. E. Biagi, M. Brenci, S. Fontani, L. Masotti, and M. Pieraccini, "Photoacoustic generation: optical fiber ultrasonic sources for non-destructive evaluation and clinical diagnosis," Opt. Rev. **4**(4), 481–483 (1997).
3. P. A. Fomitchov, A. K. Kromine, and S. Krishnaswamy, "Photoacoustic probes for nondestructive testing and biomedical applications," Appl. Opt. **41**(22), 4451–4459 (2002).
4. V. Giurgiutiu, *Structural health monitoring with piezoelectric wafer active sensors* (Elsevier, 2008).
5. E. Biagi, F. Margheri, and D. Menichelli, "Efficient laser-ultrasound generation by using heavily absorbing films as targets," IEEE Trans. Ultrason. Ferroelectr. Freq. Control **48**(6), 1669–1680 (2001).
6. V. Kochergin, K. Flanagan, Z. Shi, M. Pedrick, B. Baldwin, T. Plaisted, B. Yellampalle, E. Kochergin, and L. Vicari, "All-fiber optic ultrasonic structural health monitoring system," Proc. SPIE **7292**, 72923D, 72923D-8 (2009).
7. C. I. Swift, S. G. Pierce, and B. Culshaw, "Generation of an ultrasonic beam using imbedded fiber optic delivery and low power laser sources," Proc. SPIE **3986**, 20–26 (2000).
8. S. Baek, Y. Jeong, and B. Lee, "Characteristics of short-period blazed fiber Bragg gratings for use as macro-bending sensors," Appl. Opt. **41**(4), 631–636 (2002).
9. T. Guo, L. Y. Shao, H. Y. Tam, P. A. Krug, and J. Albert, "Tilted fiber grating accelerometer incorporating an abrupt biconical taper for cladding to core recoupling," Opt. Express **17**(23), 20651–20660 (2009).
10. L. Y. Shao, L. Y. Xiong, C. K. Chen, A. Laronche, and J. Albert, "Directional bend sensor based on re-grown tilted fiber Bragg grating," J. Lightwave Technol. **28**(18), 2681–2687 (2010).
11. R. J. Von Gutfeld and H. F. Budd, "Laser-generated MHz elastic-waves from metallic-liquid interfaces," Appl. Phys. Lett. **34**(10), 617–619 (1979).
12. T. Buma, M. Spisar, and M. O'Donnell, "High-frequency ultrasound array element using thermoelastic expansion in an elastomeric film," Appl. Phys. Lett. **79**(4), 548–550 (2001).
13. H. Yang, J. S. Kim, S. Ashkenazi, M. O'Donnell, and L. J. Guo, "Optical generation of high frequency ultrasound using two-dimensional gold nanostructure," Appl. Phys. Lett. **89**(9), 093901 (2006).
14. H. Won Baac, J. G. Ok, H. J. Park, T. Ling, S. L. Chen, A. J. Hart, and L. J. Guo, "Carbon nanotube composite optoacoustic transmitters for strong and high frequency ultrasound generation," Appl. Phys. Lett. **97**(23), 234104 (2010).
15. Q. Zhang, N. Liu, T. Fink, H. Li, W. Peng, and M. Han, "Fiber-optic pressure sensor based on π-Phase-shifted fiber Bragg grating on side-hole Fiber," IEEE Photon. Technol. Lett. **24**(17), 1519–1522 (2012).

#184391 - $15.00 USD Received 28 Jan 2013; revised 24 Feb 2013; accepted 24 Feb 2013; published 4 Mar 2013
(C) 2013 OSA

16. K. P. Chen, B. McMillen, M. Buric, C. Jewart, and W. Xu, "Self-heated fiber Bragg grating sensors," Appl. Phys. Lett. **86**(14), 143502 (2005).
17. J. D. Andrade, R. A. Vanwagenen, D. E. Gregonis, K. Newby, and J. N. Lin, "Remote fiber-optic biosensors based on evanescent-excited fluoro-immunoassay - concept and progress," IEEE Trans. Electron. Dev. **32**(7), 1175–1179 (1985).

1. Introduction

Active ultrasonic testing is a powerful tool for medical diagnosis, material characterization and structural health monitoring [1–4]. It uses ultrasonic transducers and sensors to actively excite the structure and, in the meantime, measure its ultrasonic response for detecting the presence or extent of structural defects. With permanently imbedded transducers, active ultrasonic testing can provide real-time, on-demand accessing with reduced cost on the structural health status. Currently, piezoelectric transducers (PZTs) are the option for embedded, distributed applications. However, PZTs are relatively bulky, susceptible to electromagnetic interference, and each transducer requires two electric wires for power supply and data transmission. These disadvantages lead to significant limitations on the reliability and the number of transducers that can be imbedded in a structure. These disadvantages can be overcome by fiber-optic transducers [2, 3, 5–7]. For embedded applications, optical fiber is used to deliver the optical power to the location of interest to induce thermoelastic expansion in the material for laser ultrasound generation. Only modest optical power is required to ensure the operation in the thermoelastic region for non-destructive testing. Both single-mode fibers and multimode fiber (MMF) have been demonstrated for optical power delivery.

Despite the technical advancement in fiber-optic ultrasonic transducers, nearly all the reported configurations can only generate ultrasound at a single location of the fiber end. Few attempts have been made for ultrasonic generation at multiple points of a fiber toward all-fiber-optic ultrasonic testing system, but with limited success. The difficulty is mainly from the lack of a smart way to efficiently tap out the light from the fiber at selected locations. For example, a straightforward way is to polish the cladding area all the way to the core and replace with absorption coatings at selected locations of a MMF for ultrasonic generation [6]. In such a configuration, each of the transducers cannot be excited independently and only uses a portion of the laser light for ultrasonic generation, significantly limiting the number of transducers that can be multiplexed in a fiber and the strength of the generated ultrasound. In this paper, we propose and demonstrate a novel approach that can efficiently make use of the optical power and generate ultrasound at multiple locations along the fiber in a controllable manner.

2. Principle of operation

The approach, schematically shown in Fig. 1(a), is based on the ghost mode of a tilted fiber Bragg grating (TFBG) [8–10]. Besides the Bragg reflection of the core mode, a TFBG can convert the forward-propagating core mode to a number of back-propagating cladding modes at wavelengths determined by the effective refractive indices of the corresponding cladding modes, as illustrated in Fig. 1(b). When the tilted angle is relatively small (< 5°), the TFBG converts the core mode of the fiber to a group of low-order cladding modes at a wavelength close to the Bragg wavelength (this group of modes is usually referred to as "ghost mode" because its distinguished coupling strength and spectral position compared to other cladding mode coupling) [9]. A series of strong TFBGs are fabricated on the fiber in such a way that a downstream TFBG always has a longer ghost mode wavelength than the Bragg wavelength of the neighboring upstream TFBG, as illustrated in Fig. 1(c). Such configuration will ensure that the laser light can be completely tapped out of the core and into the cladding of the fiber only at the position of the TFBG whose ghost wavelength is the same as the laser wavelength. For ultrasonic generation, as shown in Fig. 1(d), a section of the fiber cladding before the TFBG is partially removed and replaced with laser-responsive, ultrasonic-generating materials, such as metal films [11], polymer composite [12], gold nanoparticles arrays [13], and carbon nanotube composite [14]. Because the core mode is well confined at the center of

#184391 - $15.00 USD Received 28 Jan 2013; revised 24 Feb 2013; accepted 24 Feb 2013; published 4 Mar 2013
(C) 2013 OSA

the fiber while the ghost mode spread out to the whole cross-section of the fiber, as shown in Fig. 1(e), the cladding removal and ultrasonic-generating material can absorb the ghost mode with high efficiency and have little effect on the core-mode propagation. As a result, the laser corresponding to the wavelength of a ghost mode passes through all the upstream TFBGs until it reaches the TFBG of the ghost mode and is tapped out of the fiber for ultrasound generation at that particular location. It is clear that the number of TFBGs that can be multiplexed is determined by the range of the operational wavelength and the spectral separation of the ghost mode and the Bragg reflection mode of each TFBG. The spectral separation between the ghost mode and the Bragg reflection for a TFBG with small tilt angles is typically < 2 nm.

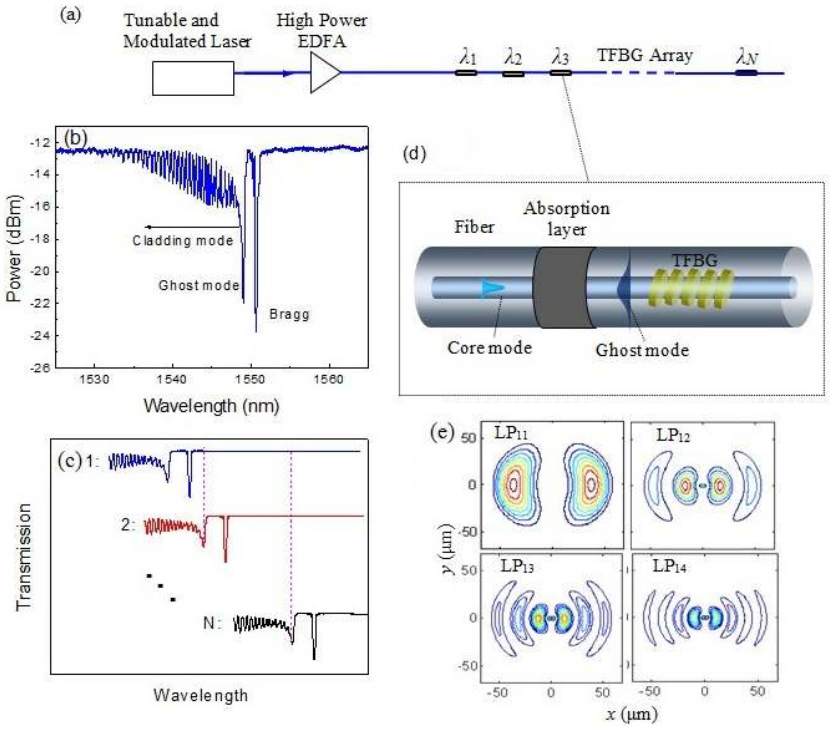

Fig. 1. Conceptual illustration of the distributive fiber-optic laser-ultrasound generation. **a,** Schematic of the proposed system. **b,** Transmission spectrum of a TFBG showing the Bragg reflection, ghost mode and cladding mode coupling. **c,** Laser-ultrasound generation by the ghost mode tapping out of the fiber that induces thermoelastic expansion of the absorption layer. **d,** TFBG spectrum arrangement to ensure that the light power is tapped out only at selected locations depending on the laser wavelength. **e,** Numerically-simulated mode-intensity distributions of the four cladding modes (LP_{11}, LP_{12}, LP_{13}, and LP_{14}) that form the ghost mode of a 4° TFBG in a 125 μm regular single-mode fiber [9].

3. Experimental results

The proposed approach was demonstrated using a set up schematically shown in Fig. 2(a). Using a 193 nm UV laser and phasemasks [15], three TFBGs were fabricated on regular single-mode fibers (SMF-28), namely BG1, BG2, and BG3, whose ghost mode wavelengths were located at 1544.1, 1548.9, and 1555.2 nm, respectively. Each TFBG was 5.5 mm long and had a tilt angle of 2°. They were connected sequentially along a fiber approximately 1 m apart from each other. As discussed earlier, such arrangement ensures that upstream TFBGs do not affect the ultrasound generation from downstream TFBGs. A short section of fiber approximately 5 mm long before each of BG2 and BG3 were etched with 50 w.t. % hydrofluoric (HF) acid to reduce the fiber diameter and facilitate the ghost mode tapping. The

#184391 - $15.00 USD Received 28 Jan 2013; revised 24 Feb 2013; accepted 24 Feb 2013; published 4 Mar 2013
(C) 2013 OSA

fiber diameter was reduced to ~60 μm from 125 μm with a transient length of ~560 μm, as shown in Fig. 2(f). Note that the reduced fiber diameter is still much larger than the mode field diameter (~10.4 μm) of the core mode and does not affect its propagation. The etched region of the fiber was then buried into a 200 μm deep slot pre-machined on an aluminum plate using a mixture of fine graphite powder (−200 mesh) and epoxy resin (Duralco: 4460) that was subsequently cured at a temperature of 120 °C for 4 hours, as shown in Fig. 2(e). The cured graphite/epoxy mixture also serves as the highly absorptive material with large thermal expansion coefficient for efficient laser-ultrasound generation. The transmission spectrum of three gratings in the setup is shown in Fig. 2(c), clearly showing the wavelength positions of the ghost mode coupling and Bragg reflections. The spectral separation between the ghost mode and the Bragg reflection for each TFBG is approximately 1.7 nm. The wavelengths of the Bragg reflections are further confirmed by the reflection spectrum of the three TFBGs shown in Fig. 2(d). Two pulsed seed fiber lasers, whose wavelengths are centered at 1549.3 and 1555.9 nm, were used for ultrasound generation at BG2 and BG3, respectively. The light from the seed laser were amplified by a high-power erbium-doped-fiber-amplifier (EDFA) before launching to the fiber. To account for the slight difference between the ghost mode wavelengths and the laser wavelengths, a translation stage was used for each grating to tune the ghost mode wavelength with the help from an optical spectrum analyzer (OSA) by stretching the fiber, as schematically shown in Fig. 2(b). Note that, in real applications, the wavelength tuning of the TFBGs may not be necessary if wavelength tunable lasers or laser sources whose wavelengths match the wavelengths of the ghost modes of the TFBGs are used. The generated ultrasound was detected by a PZT ultrasonic sensor (Panametrics V122) mounted underneath the buried fiber on the opposite side of the aluminum plate. The PZT sensor has a resonant frequency of 7.5 MHz.

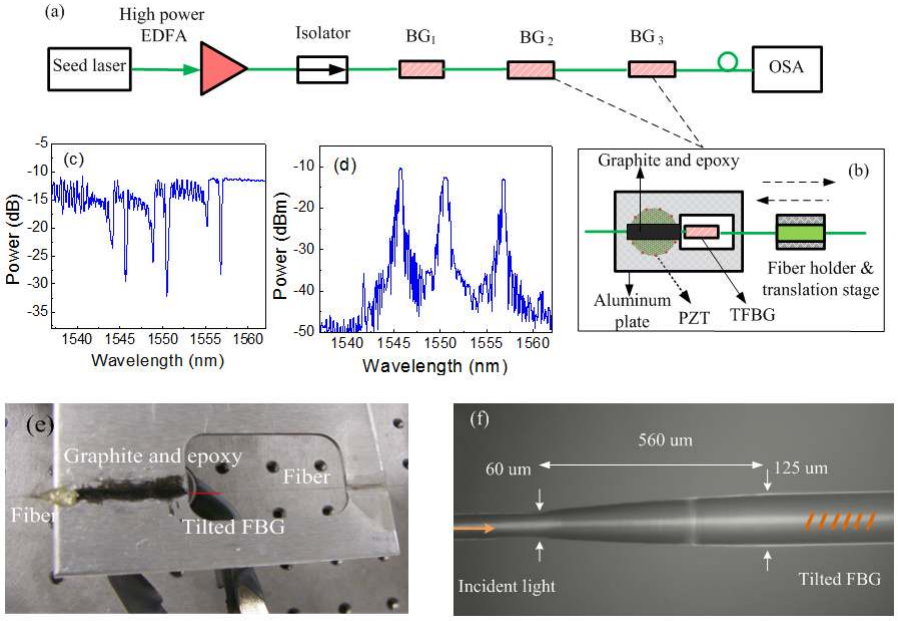

Fig. 2. Experimental demonstration. **a,b,** Schematic of the experimental setup. **c, d,** Transmission spectrum **(c)** and reflection spectrum **(d)** of the three TFBGs. **e,** Picture of one of the laser-ultrasound generation nodes. **f,** Picture of an etched fiber before a TFBG for tapping out the ghost mode.

#184391 - $15.00 USD Received 28 Jan 2013; revised 24 Feb 2013; accepted 24 Feb 2013; published 4 Mar 2013
(C) 2013 OSA

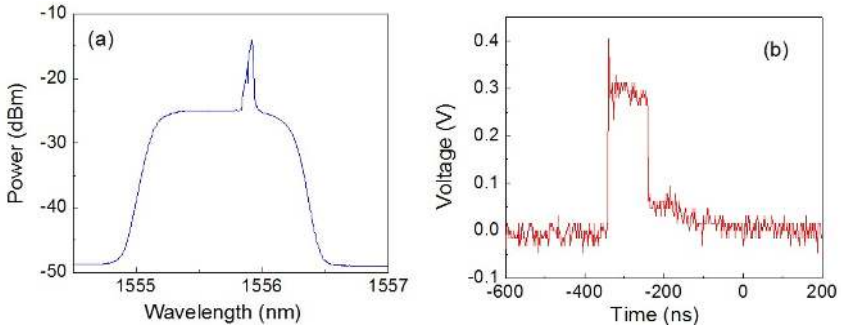

Fig. 3. Laser characteristics. **a,** Seed laser spectrum. **b,** Laser pulse measured after the EDFA.

We studied the ultrasound generation from BG3 first. The optical pulses from the 1555.9 nm laser with a repetition rate of 3 kHz and pulse width of ~100 ns were amplified by the EDFA to an average optical power of 1 W before launching into the fiber. Figures 3(a) and 3(b) show the spectrum of the seed laser measured by the OSA and the laser pulse after the EDFA measured by a photodetector and an oscilloscope. The energy of each of the optical pulses after the EDFA is estimated to be 0.33 mJ. Because the BG3 ghost mode wavelength is slightly shorter than the laser wavelength, the laser is transmitted through the fiber, as indicated by the spectrum measured at the fiber end shown in Fig. 4(a) which is similar to original laser spectrum shown in Fig. 3(a). Then the ghost mode wavelength was tuned to match the laser wavelength by stretching the fiber with the translation stage. Evidenced by the spectrum shown in Fig. 4(b), the laser was coupled to the ghost mode and ultrasound was detected with the PZT sensor. Figure 4(d) is the ultrasound signal detected by the PZT, which is a series of narrow ultrasonic pulses with the same repetition rate (3 kHz) of the laser pulses. The detail of an ultrasonic pulse is shown in Fig. 4(e) and its Fourier transform shown in Fig. 4(f) reveals that the generated ultrasound had a broad and relatively flat spectrum below 8 MHz. As the fiber was further stretched so that the ghost mode was longer than the laser wavelength, in which case the transmission spectrum of the laser is shown in Fig. 4(c), no ultrasound was detected. Note that, due to the high optical power of the EDFA output, an optical loss was intentionally introduced to the fiber link by coiling the fiber right before the OSA [see Fig. 2(a)] when the spectra shown in Figs. 4(a)-4(c) were measured.

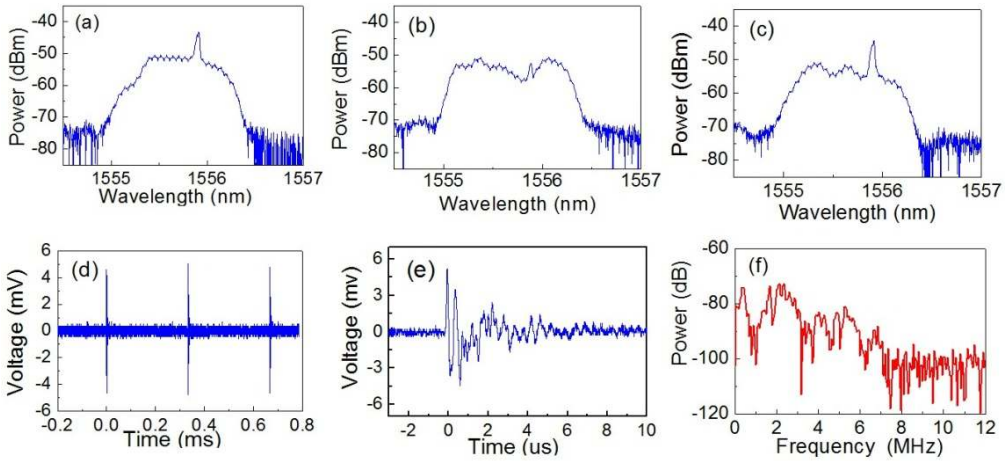

Fig. 4. Experimental results. **a-c,** Laser spectrum measured after the three TFBGs when the ghost mode of the BG3 was tuned to be shorter than (**a**), equal to (**b**), and longer than (**c**) the laser peak wavelength. **d** Ultrasonic signal pulses generated by BG3 and detected by a PZT sensor. Signal was averaged over 10 measurements. **e,** Enlarged view of an ultrasonic pulse in (**d**). **e,** Fourier transform of the data shown in (**f**).

#184391 - $15.00 USD Received 28 Jan 2013; revised 24 Feb 2013; accepted 24 Feb 2013; published 4 Mar 2013
(C) 2013 OSA

To demonstrate distributive ultrasound generation, the seed laser was replaced with the 1549.3 nm laser whose wavelength was close to the ghost mode wavelength of BG2. Ultrasound signal was detected by the PZT sensor at the location of BG2 when its ghost mode wavelength of BG2 is tuned to match the laser wavelength. The results, including the 3 kHz ultrasonic pulse train, the detailed view of an ultrasonic pulse, and its Fourier transform, are shown in Figs. 5(a), 5(b) and 5(c), respectively. They are similar to those generated from BG3.

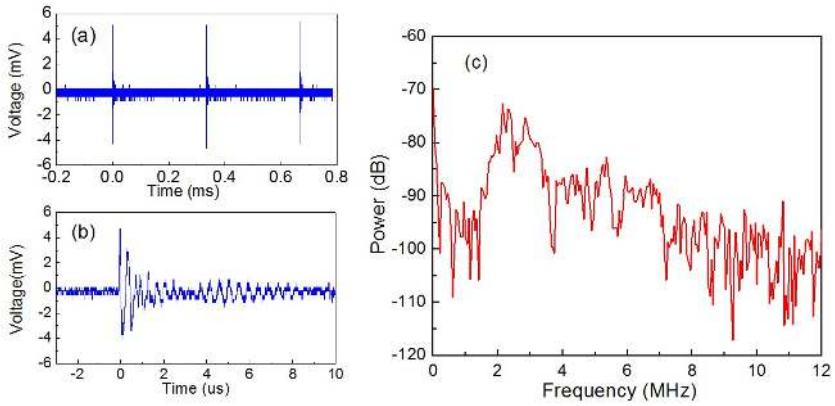

Fig. 5. **a,** Ultrasonic signal pulses generated by BG2 and detected by a PZT sensor. Signal was averaged over 10 measurements. **b,** Enlarged view of an ultrasonic pulse in (**a**). **c,** Fourier transform of the data shown in (**b**).

4. Conclusion

We have proposed and demonstrated a smart light tapping scheme which can only couple the light of a given wavelength out of the fiber and allow the light of longer wavelength pass by without loss. Using this light tapping scheme, we experimentally demonstrated, for the first time, efficient and distributive laser-ultrasound generation at multiple locations along a fiber in a controllable manner, which may find attractive applications in all-fiber and embedded ultrasonic testing system for structural health monitoring. The proposed light tapping method can also find applications in remote fiber device actuation [16] and distributed biochemical sensing [17].

Acknowledgment

This work was supported in part by the Office of Naval Research under grants N000141110705 and N000141110262, and the National Science Foundation under grant EPS-1004094. The authors would like to thank Dr. Joseph Turner (University of Nebraska-Lincoln) for his assistance in the ultrasound detection.

#184391 - $15.00 USD Received 28 Jan 2013; revised 24 Feb 2013; accepted 24 Feb 2013; published 4 Mar 2013
(C) 2013 OSA